24th INTERNATIONAL CONGRESS ON SOUND AND VIBRATION
23–27 July 2017, London

ERROR ANALYSIS AND EXPERIMENTAL INVESITATION OF THE MAPPING RELATIONSHIP BASED NAH WITH SPHERICAL SOLUTION

Haijun Wu, Weikang Jiang

State Key Laboratory of Mechanical System and Vibration, Shanghai Jiao Tong University, Shanghai 200240, China
Institute of Vibration, Shock and Noise, Collaborative Innovation Center for Advanced Ship and Deep-Sea Exploration, Shanghai Jiao Tong University, Shanghai 200240, China
email: haijun.wu@sjtu.edu.cn, wkjiang@sjtu.edu.cn ,

A mapping relationship based near-field acoustic holography was proposed previously. It requires an enclosing measurement to form the unique mapping relationship between the vibrating structure and the hologram. A guideline was developed to choose the necessary number of the fundamental solution as well as set up the microphone array in an optimized way. The NAH is an inverse problem and thus poses significant challenges to the stable and accurate solution. And, a practical measurement is prone to errors and always incorporates uncertainties, such as random fluctuations, effect of rapid decay of the evanescent waves. To investigate the influence of errors on the performance of the MRS-based NAH, the errors are divided into two parts. One is truncation error introduced in the modal decomposition, and another one is the noise included in the experiment. An expression of the relative error of the reconstructed pressure energy is derived based on the two types of errors. An approach is developed to estimate the lower and upper bounds of the relative error. It gives a guide to predict the error for a reconstruction under the condition that the truncation error and the signal-to-noise ratio are given. Numerical examples with different kinds of errors are elaborately designed to validate the stability as well as the correctness of the error analysis. At last, the MRS-based NAH is further examined and verified by a physical experiment. A satisfied agreement with the directly measured pressure on a validation surface is observed for both quantity and distribution of the reconstructed pressure.

Keywords: near-field acoustic holography, mapping relationship, experimental study, spherical fundamental solutions

1. Introduction

Near-field acoustic holography (NAH) is an effective tool to reconstruct the interested acoustic quantities (e.g. sound pressure, particle velocity) based on a number of measurements at a close distance to a structure which are typically returned by an array microphones or probes. As is well known, it is usually claimed as an ill-posed problem in the sense of Hadamard [1], i.e. it may have no solution at all or the solution may not be unique and it may be extremely sensitive to slight errors in the input. It is due to that the inverse operator is ill-conditioned, e.g. subject to larger condition number, which are generally caused by the over selected basises in either numerical or analytical form for the description of acoustic quantities on the surface of structure or hologram.

To circumvent this issue, regularization methods were introduced to the NAH. The prevailing approach goes to the popular Tiknonov regularization which controls the solution by balancing the fidelity term and the regularization errors [1-5]. Thus, several strategies had been developed to properly

determine the regularization parameter, such as generalized cross validation (GCV) [6] and the L-curve [7], etc. However, at present, there is still no absolutely universal method that is robust enough and always produces a good regularization parameter. Sometimes the very ill-posed inverse operator makes the regularization a real difficulty, and in turn is very urgent to need a proper regularization method. The ill-poseness is even more serious for incomplete measurement regardless the types of NAH adopted, such as the attempts to reconstruct the acoustic quantities on a three dimensional structure from one or several non-enclosing holograms. While the exact solution is possible to be obtained for the inverse operation from a measurement on a complete hologram enclosing the vibrating structure [8, 9]. It is the measurement that can form a unique one-to-one mapping relationship between the surface of structure and hologram [10].

Few works are devoted to the error analysis of the NAH by comparing with that for the regularization methods. It is because the NAH was usually viewed as a very ill-posed inverse problem for which obtaining a regularized solution is the primary task. Thus, it is difficult to predict or estimate the reconstruction accuracy. Instead of a predictable way, numerical simulation and experimental validation are two frequently adopted methods to investigate the performance of NAH for different parameters [11-13]. For practical problems, it is hard to estimate the accuracy of the reconstructed results. In this work, the error analysis and experimental study of the MRS-based NAH [10] are reported.

2. Error analysis of the MRS-based NAH

On the holograms, the error included pressure is simply modelled as

$$\mathrm{p}(\mathbf{x}) = \mathrm{p}_0(\mathbf{x}) + \mathrm{n}(\mathbf{x}), \text{ or } \mathbf{P} = \mathbf{P}_0 + \mathbf{n} \tag{1}$$

, where $\mathbf{P_0}$ represents the source pressure and $\mathbf{n}$ is the noise terms. Denote the signal to noise ratio (SNR) on the hologram as

$$\mathrm{SNR} = 10\log_{10}\frac{W_{P_0}}{W_{Noise}} = 10\log_{10}\frac{\int_{S_h}|\mathrm{P}_0(\mathbf{x})|^2 dS(\mathbf{x})}{\int_{S_h}|\mathrm{n}(\mathbf{x})|^2 dS(\mathbf{x})} \tag{2}$$

, where W_{P_0} and W_{Noise} represent energies of source pressure and noise pressure, respectively. Under the condition that the source pressure and noise pressure can be completely decomposed by a set of normalized modes, the SNR can be reformatted by the Parseval law as

$$\mathrm{SNR} = 10\log_{10}\frac{\|\boldsymbol{\alpha}_0\|_2^2}{\|\boldsymbol{\alpha}_{Noise}\|_2^2} \tag{3}$$

in which $\boldsymbol{\alpha}_0$ and $\boldsymbol{\alpha}_{Noise}$ are coefficients of the locally normalized orthogonal patterns on the hologram for the source pressure and noise term, and correspondingly the coefficients for pressure $\mathbf{P}$ is $\boldsymbol{\alpha} = \boldsymbol{\alpha}_0 + \boldsymbol{\alpha}_{Noise}$.

The participant coefficients of the FS modes S_i (Eq.(4) in Ref. [14]) can be obtained indirectly as

$$\lambda_i = \sum_{j=i}^{\infty} R_{ij}\alpha_j \text{ or } \boldsymbol{\lambda} = \mathbf{R}\boldsymbol{\alpha} \tag{4}$$

in which

$$\alpha_j = \langle p(\mathbf{x}), e_j(\mathbf{x})\rangle_{S_h} \tag{5}$$

are participant coefficients for the normalized and orthogonal modes $e_j(\mathbf{x})$, and the normalized mode is related to the FS by

$$\mathbf{E} = \mathbf{SR} \tag{6}$$

, where the orthogonal and normalized modes $\mathbf{E} = [e_1(\mathbf{x}), e_2(\mathbf{x}), \cdots]$, $\mathbf{S} = [S_1(\mathbf{x}), S_2(\mathbf{x}), \ldots] = [S_0^0(\mathbf{x}), S_1^{-1}(\mathbf{x}), S_1^0(\mathbf{x}), \cdots]$ is a row lined FS and $\mathbf{R}$ is an upper triangular square matrix.

Once the participant coefficients is obtained on the hologram, reconstruction process is a simple series evaluation as

$$p(\mathbf{x}) = \sum_{i=0}^{\infty} \lambda_i S_i(k, \mathbf{x}) \text{ for } \mathbf{x} \in \Gamma \text{ or } \mathbf{p}_\Gamma = \boldsymbol{S}_\Gamma \boldsymbol{\lambda} \tag{7}$$

where $\mathbf{p}_\Gamma$ and $\boldsymbol{S}_\Gamma$ are reconstructed pressure and FS on the surface of the vibrating structure, respectively. Decompose the FS on the surface of vibrating structure $\boldsymbol{S}_\Gamma$ as

$$\boldsymbol{S}_\Gamma = \mathbf{E}_\Gamma \mathbf{R}_\Gamma^- \tag{8}$$

where $\mathbf{E}_\Gamma$ is the column normalized modes on the surface of vibrating structure, and $\mathbf{R}_\Gamma$ is a translation operator which is an upper triangular square matrix. Reconstructed sound pressure on the surface of the vibrating structure, can be expressed as

$$\mathbf{p}_\Gamma = \mathbf{E}_\Gamma \mathbf{R}_\Gamma^- \mathbf{R} \boldsymbol{\alpha} \tag{9}$$

According to the Parseval law, the reconstructed pressure energy on the surface of vibrating structure is

$$W_{P_\Gamma} = \|\mathbf{R}_\Gamma^- \mathbf{R} \boldsymbol{\alpha}\|_2^2 = \boldsymbol{\alpha}^* \mathbf{T}_\mathbf{R} \boldsymbol{\alpha} \tag{10}$$

, where $\mathbf{T}_\mathbf{R} = \mathbf{R}^* \mathbf{R}_\Gamma^{-*} \mathbf{R}_\Gamma^- \mathbf{R}$ is a Hermitian matrix. Therefore, there is an eigendecomposition of $\mathbf{T}_\mathbf{R} = \mathbf{Q}^* \boldsymbol{\Lambda} \mathbf{Q}$ in which $\mathbf{Q}$ is a unitary complex matrix whose columns comprise an orthonormal basis of the eigenvectors of $\mathbf{T}_\mathbf{R}$, and $\boldsymbol{\Lambda}$ is a real diagonal matrix whose main diagonal entries are the corresponding eigenvalues. Assume the eigenvalues are sorted in a descending order, such as $\Lambda_i \geq \Lambda_j$ for $j > i$. The lower and upper bounds of the reconstructed pressure energy are easy to be obtained

$$\Lambda_d \|\boldsymbol{\alpha}\|_2^2 \leq W_{P_\Gamma} \leq \Lambda_1 \|\boldsymbol{\alpha}\|_2^2 \tag{11}$$

, where d is the dimension of the matrix. In practice, the relative error of reconstructed pressure energy on the surface of the vibrating structure is more concerned. Obviously, the bounds of the exact pressure energies $W_{P_{0,\Gamma}}$ and noise generated pressure energies $W_{P_{\text{Noise},\Gamma}}$ can be obtained with coefficients $\boldsymbol{\alpha}$ replaced with $\boldsymbol{\alpha}_0$ and $\boldsymbol{\alpha}_{Noise}$ in Eq. (11), respectively. Thus, bounds for the relative errors $\varepsilon_{W_\Gamma} = W_{P_{\text{Noise},\Gamma}} / W_{P_{0,\Gamma}}$ are

$$cond(\mathbf{T}_\mathbf{R})^{-} 10^{-SNR/10} \leq \varepsilon_{W_\Gamma} \leq cond(\mathbf{T}_\mathbf{R}) 10^{-SNR/10} \tag{12}$$

where $10^{-SNR/10} = \|\boldsymbol{\alpha}_{Noise}\|_2^2 / \|\boldsymbol{\alpha}_0\|_2^2$, and $cond(\mathbf{T}_\mathbf{R}) = \boldsymbol{\Lambda}_1 / \boldsymbol{\Lambda}_d$ is the condition number of the translator matrix $\mathbf{T}_\mathbf{R}$. Eq. (12) can be rewritten as

$$SNR - 10 \log_{10} cond(\mathbf{T}_\mathbf{R}) \leq SNR_\Gamma \leq SNR + 10 \log_{10} cond(\mathbf{T}_\mathbf{R}) \tag{13}$$

in which $SNR_\Gamma = -10 \log_{10} \varepsilon_{W_\Gamma}$ is the signal to noise ratio of the reconstructed pressure on the model's surface.

Above analysis is based on an assumption that the pressure can be completely decomposed by a set of modes. Otherwise, the Parseval law cannot be applied equivalently in evaluating the pressure energy. However, the complete set of modes is hardly to be satisfied in decomposing the radiated pressure of a realistic radiator, alternatively an incomplete set is applied to approximately decompose the radiated pressure within a given tolerance. Therefore, a compromise on accuracy and robustness is made by truncating the series expansion, Eq.(7), with a proper number *N*. Due to the truncation, the measured pressure energy evaluated by the modal decomposition method on holograms is not equal to the true quantities, and so is the noise energy.

Suppose the exact pressure on the surface of the vibrating structure is $p_{0,\Gamma}$ and the corresponding reconstructed pressure is p_Γ. Therefore, the relative error of the reconstructed pressure energy is

$$\varepsilon_{W_\Gamma} = \frac{\|\mathbf{p}_{0,\Gamma} - \mathbf{p}_\Gamma\|_2^2}{\|\mathbf{p}_{0,\Gamma}\|_2^2} \tag{14}$$

According to the derivation in the appendix in the Ref. 15, the relative error ε_{W_Γ} can be expressed as

$$\varepsilon_{W_\Gamma}(c_1, c_2, c_3, c_4) = \frac{c_4 + c_3 10^{-SNR/10} + c_1 \sqrt{c_4} \sqrt{c_3} 10^{-SNR/20}}{1 + c_4 + c_2 \sqrt{c_4}} \tag{15}$$

It reaches the lower bound at $c_1 = -2$ and $c_2 = 2$, and the upper bound at $c_1 = 2$ and $c_2 = -2$. However, Eq. (15) is a nonlinear function for variables c_3. A constrained nonlinear optimization algorithm is adopted to find the lower and upper bounds, as the minimum of a problem specified by

$$\min_{(c_3)} f(c_3) \; such\ that\ cond(\mathbf{T_R})^- \le c_3 \le cond(\mathbf{T_R}) \tag{16}$$

, where the objective function is

$$f(c_3) = \begin{cases} \varepsilon_{W_\Gamma}(-2,2,c_3,c_4), & for\ lower\ bound \\ -\varepsilon_{W_\Gamma}(2,-2,c_3,c_4), & for\ upper\ bound \end{cases} \tag{17}$$

In the above analysis, the variables SNR and c_4 are supposed to be given. The SNR of the environment can be estimated by measurement. For the ideal case in which there is no noise included, equivalent to SNR $= \infty$, the lower bound of the relative error is easy to be obtained as

$$\varepsilon_{W_\Gamma} \ge \frac{c_4}{1 + c_4 + 2\sqrt{c_4}} \tag{18}$$

, which is only related to the c_4 and in turn related to the number of adopted participant modes. The actual reconstructed error of a realistic problem or a case with small SNR is not expected to have a lower bound less than that estimated for no noise included case. Thus, the lower bound of the reconstructed pressure energy can be estimated by Eq. (18).

3. Numerical Simulations

In this section, numerical examples are set up to investigate the performance of the MRS-based NAH on different types of measurement configurations with noise included. In the following simulations, the edge length of the cube is set as $a = 0.2$ m as shown in Figure 2. The setup is schematically illustrated in Figure 1, the spherical hologram is away from the equivalent radius $\tilde{r} = \sqrt{S/4\pi}$ where S is the area of the cubic model by Δ.

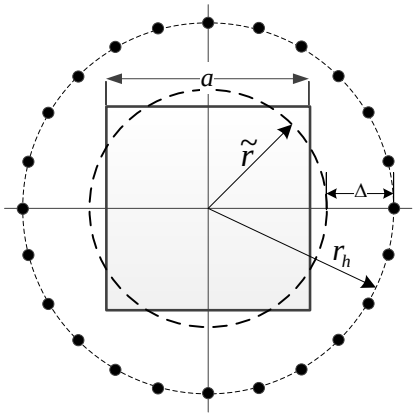

Figure 1 Schematic setup for top view of the spherical hologram

The radiated source pressure of the cube is computed by the boundary element method (BEM) with the normal velocity supplied by the finite element method (FEM). The number of modes is estimated by the method introduced in Section 2.2 in the Ref. 15. It is to simulate the realistic radiator whose exact number of efficient modes is hardly to be obtained but estimated by a reasonable guideline. A specific amount of noise with prescribed SNR on the hologram, which is generated with

$$\mathbf{n} = \gamma \mathbf{S} \boldsymbol{\lambda}_{Noise} \tag{19}$$

where $\boldsymbol{\lambda}_{Noise}$ is a Gaussian random vector, and $\gamma = 10^{-SNR/20} \|\mathbf{R}^{-1}\boldsymbol{\lambda}_{Noise}\|_2^- \sqrt{W_{P_0}}$ is an energy related variable to make sure the generated noise $\mathbf{n}$ can make the specified SNR.

To simulate more realistic problems in which the necessary number of participant modes is hard to be obtained exactly and the truncation error is introduced, the radiated source pressure on holograms

is generated from a vibrating cubic structure driven by a harmonic excitation. As shown in Figure 2, the cubic model is excited by a harmonic force along z-axial at a specified position $(0.4a, 0.4a, -0.5a)$ and the four corners at the bottom are constrained. Thicknesses of the six walls are set as 0.004 m, and steel material is assigned to the model. The harmonic response is obtained by a commercial finite element software at frequencies 601Hz, which is chosen closely to the one modal frequencies with an aim to obtain a uniformly distributed velocity on the surface. Once the boundary velocities are obtained, the radiated sound pressure at the measurement positions are computed by the boundary element method [15] as the inputs for the reconstruction.

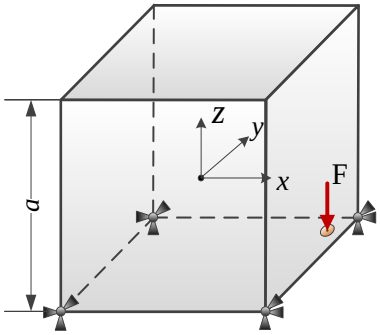

Figure 2 Configuration of the cubic structure excited by a harmonic force F (denoted by the red arrow) along the z-axis

There are errors due to the truncation of the participant modes. Therefore, reconstructions are firstly performed for the pressure $\boldsymbol{p}_{num}$ obtained numerically by the FEM and BEM which is also treated as the exact source pressure. The reconstructions are considered as the references of no-noise included measurement. Contour plots of the reconstructed pressure for the reference cases are given in Figure 3. In spite of a slight disparity in the quantity, it can be observed that the reference reconstructions are very satisfied with the simulated pressure because the significant pressure distributions are well reconstructed. Later on, different SNRs ranging from 4dB to 28dB with the increment being 4dB are added to the simulated pressure to validate the robustness of the NAH to the noise which is unavoidable in the realistic experiment. The noise is also obtained by Eq. (19).

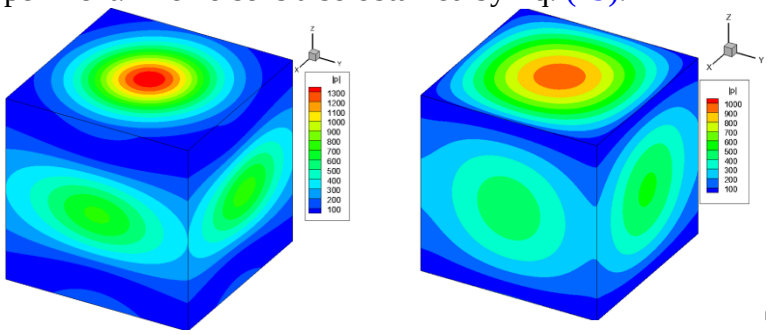

(a) (b)

Figure 3 The reconstructed pressure based on the no-noised included measurement on (a) the spherical holograms with the necessary number of modes N=3 for (b) the simulated results at frequency 601Hz

Relative errors of reconstructed pressure energy on the model's surface is defined as

$$\varepsilon_{W_\Gamma} = \frac{\|\boldsymbol{p}_{recon} - \boldsymbol{p}_{num}\|_2^2}{\|\boldsymbol{p}_{num}\|_2^2} \tag{20}$$

, where $\boldsymbol{p}_{recon}$ is the reconstructed pressure based on different SNRs. The relative errors are plotted in Figure 4. To estimate the error, variable c_4 is required to be supplied by

$$c_4 = \frac{\|\boldsymbol{p}_{recon}\|_2^2}{\|\boldsymbol{p}_{recon} - \boldsymbol{p}_{num}\|_2^2} \tag{21}$$

based on the simulated results. Figure 4 depicts that the most necessary number of modes for the pressure reconstruction at frequency 601Hz is $N = 3$. The decreased results for the reconstructed

pressure with increased number of necessary modes illustrate that over-selected number of modes may result in accuracy loss especially for structures with irregular shapes as well as small SNRs. It is because that over-selected number of basises will yield the translators with larger condition numbers which is likely to amplify the errors in the experiment.

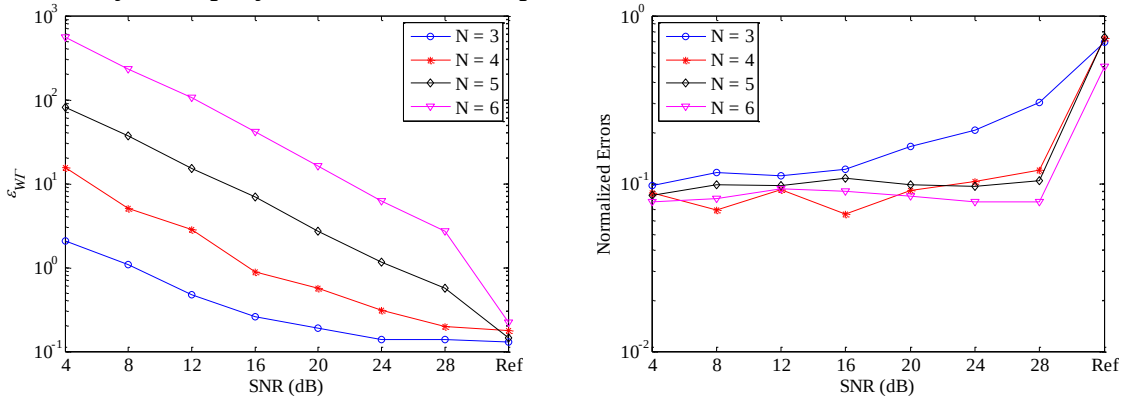

(a) (b)

Figure 4 Errors of the reconstructed pressure energy with planar holograms at 601Hz for (a) the relative error $\boldsymbol{\varepsilon_{W_T}}$, and (b) the normalized error $\tilde{\boldsymbol{\varepsilon}}_{\boldsymbol{W_T}}$

The normalized errors are also presented in Figure 4(b). The normalized errors are all less than one and increase along with the SNRs. The small errors for small SNRs and participant number of modes are due to the fact their lower bounds are underestimated while the upper bounds are over estimated. The extreme small normalized errors for the case $N = 3$ are due to the dominated truncation errors for small number of adopted participant modes. As indicated for the reference cases, also the no-noise included cases, the reconstructed errors are closer to one, or in other wards more approximated to the estimated upper bounds. More important than the cases with small SNRs for which the estimated lower bounds are almost zero, the no-noise included cases (with infinity large SNR) can supply more reasonable lower bounds with the approach in Section 2. The numerical examples clearly demonstrated the validity of the proposed estimation of the bounds.

4. Experimental Study

An experiment is set up to explore the performance of the MRS-based NAH in this section. The edge length of the cubic radiator is 0.2 m. Reconstruction is performed on the spherical hologram. As shown in the Figure 5(a), the cubic model is placed at the centre of the spherical hologram by hanging in a portal frame with a rigid hollow rod. A single point drive is applied to the model by a small exciter on the top surface, Figure 5(a). To make sure a uniform velocity distribution is generated on the surface, the analyzing frequency is selected closely to one of the modal frequencies, which is 634Hz. The model has an equivalent radius $\tilde{r} = 0.138$ m, and the measurements are performed on a spherical hologram apart from the equivalent sphere by $\Delta = 0.1$ m. The necessary degree of the FS is adopted as $= 3$. Correspondingly, the minimum required microphone along the θ and ϕ direction are 4 and 7, respectively. Here, we made an over sampling by placing 5 microphones along the θ direction, and taking 9 sequential measurements along the ϕ direction.

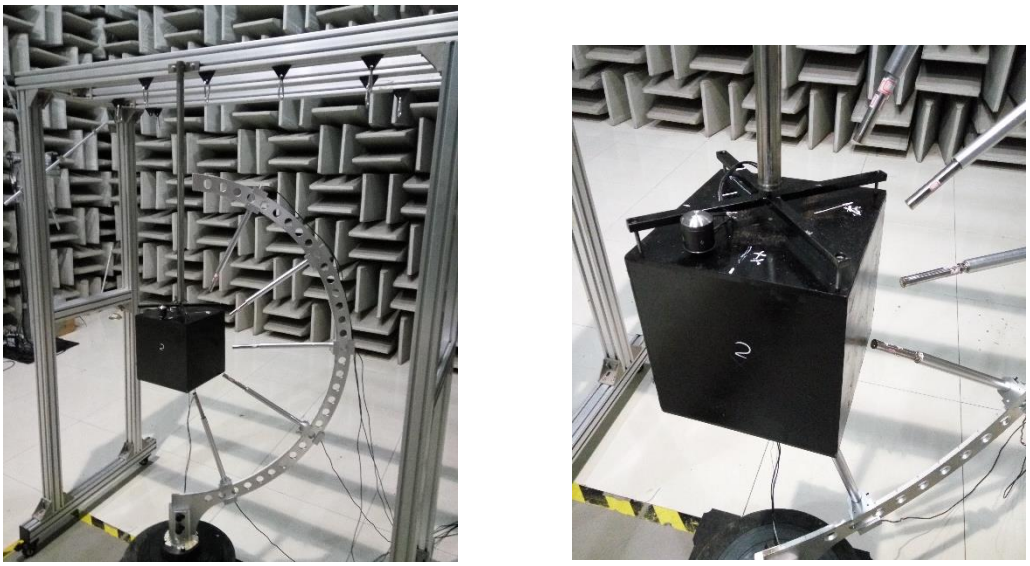

(a) (b)

Figure 5 The experimental setup: (a) overview of the configuration, (b) details of the model

To validate the reconstructed results, the same 5×9 measurements are performed on a spherical validation surface Ω with radius being 0.18 m. In light of Eq. (7), the relative difference of the reconstructed pressure with respective to the measured one on the validation surface is denoted by

$$\varepsilon_{W_\Omega} = \frac{\left\| \sum_{n=0}^{(N+1)^2} (\lambda_n - \lambda_{n,\Omega}) S_n(k,\mathbf{x}) \right\|_2}{\left\| \sum_{n=0}^{(N+1)^2} \lambda_{n,\Omega} S_n(k,\mathbf{x}) \right\|_2} \tag{22}$$

in which λ_n and $\lambda_{n,\Omega}$ are coefficients obtained on the hologram and validation surfaces, respectively. Figure 6 depicts a comparison of the radiated pressure distribution on a spherical surface between the one reconstructed from the hologram and the one measured directly on the validation surface. It is clearly observed that the reconstructed pressure has a very satisfactory distribution agreement with the measured one for which the ε_{W_Ω} is 4.5% and the relative error of the largest pressure magnitude is 21.8%.

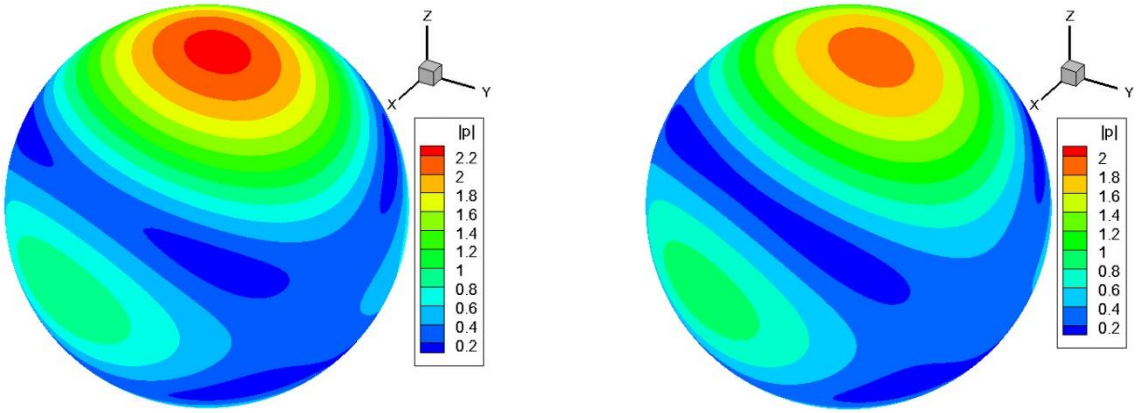

Figure 6 The radiated pressure distribution on the spherical validation surface for (a) reconstructed from the hologram, and (b) obtained from the direct measurement

5. Conclusions

In this work, error analysis as well as the experimental study of the MRS-based NAH are investigated. It is found that the reconstruction accuracy are subjected to two kinds of errors, one is the SNR and another one is the truncation error due to the limited number of participant modes adopted in the MRS-based NAH. An error model is built, and the relative error of the reconstructed pressure energy

on the surface of the vibrating structure is derived. The lower and upper bounds of the relative error can be achieved numerically by a constrained nonlinear optimization algorithm. However, the approach generally yields underestimation of the lower bound and the overestimation of the upper bound especially for MRS-NAH with large condition numbers. Alternatively, a reasonable lower bound is obtained by considering the case without noise or equivalently with positive infinite SNR. It eliminates the influence of the condition number of the inverse translator, and is only related to the truncation errors. Thus, it is feasible to predicate the lower error of a reconstruction with the MRS-based NAH once the truncation error is given, which is validated by numerical examples. Proper estimation of the truncation errors is highly related to the reasonable estimation of the lower bound, which deserves more investigation.

REFERENCES

1 Tikhonov, A. N. and Arsenin, V. I. A. *Solutions of ill-posed problems*, Winston, (1977).

2 Nelson, P. A. and Yoon, S. H. Estimation of acoustic source strength by inverse methods: Part I, conditioning of the inverse problem *Journal of Sound and Vibration*, **233** (4), 639-664, (2000).

3 Yoon, S. H. and Nelson, P. A. Estimation of acoustic source strength by inverse methods: Part II, experimental investigation of methods for choosing regularization parameters, *Journal of Sound and Vibration*, **233** (4), 665-701, (2000).

4 Kim, Y. and Nelson, P. A. Optimal regularisation for acoustic source reconstruction by inverse methods, *Journal of Sound and Vibration*, **275** (3-5), 463-487, (2004).

5 Zhang, Y. B., Bi, C. X., Xu, L. and Chen, X. Z. Novel method for selection of regularization parameter in the near-field acoustic holography, *Chinese Journal of Mechanical Engineering (English Edition)*, **24** (2), 285-292, (2011).

6 Golub, G. H., Heath, M. and Wahba, G. Generalized Cross-Validation as a Method for Choosing a Good Ridge Parameter, *Technometrics*, **21** (2), 215-223, (1979).

7 Hansen, P. C. and O'Leary, D. P. The Use of the L-Curve in the Regularization of Discrete Ill-Posed Problems, *SIAM Journal on Scientific Computing*, **14** (6), 1487-1503, (1993).

8 Valdivia, N. P., Williams, E. G. and Herdic, P. C. Approximations of inverse boundary element methods with partial measurements of the pressure field, *Journal of the Acoustical Society of America*, **123** (1), 109-120, (2008).

9 Pereira, A., Antoni, J. and Leclère, Q. Empirical Bayesian regularization of the inverse acoustic problem, *Applied Acoustics*, **97**, 11-29, (2015).

10 Wu, H. J., Jiang, W. K. and Zhang, H. B. A mapping relationship based near-field acoustic holography with spherical fundamental solutions for Helmholtz equation, *Journal of Sound and Vibration*, **373** (7), 66-88, (2016).

11 Lu, H. C. and Wu, S. F. Reconstruction of vibroacoustic responses of a highly nonspherical structure using Helmholtz equation least-squares method, *Journal of the Acoustical Society of America*, **125** (3), 1538-1548, (2009).

12 Bi, C. X. and Stuart Bolton, J. An equivalent source technique for recovering the free sound field in a noisy environment, *Journal of the Acoustical Society of America*, **131** (2), 1260-1270, (2012).

13 Bi, C. X., Hu, D. Y., Zhang, Y. B. and Bolton, J. S. Reconstruction of the free-field radiation from a vibrating structure based on measurements in a noisy environment, *Journal of the Acoustical Society of America*, **134** (4), 2823-2832, (2013).

14 Wu, H. J. and Jiang, W. K. Experimental study of the mapping relationship based near-field acoustic holography with spherical fundamental solutions, *Journal of Sound and Vibration*, **394**, 185-202, (2017).

15 Wu, H. J., Liu, Y. J. and Jiang, W. K. A low-frequency fast multipole boundary element method based on analytical integration of the hypersingular integral for 3D acoustic problems, *Engineering Analysis with Boundary Elements*, **37** (2), 309-318, (2013).